Catalysis Today 157 (2010) 143–148

Contents lists available at ScienceDirect

Catalysis Today

journal homepage: www.elsevier.com/locate/cattod

Copper grafted on SBA-15 as efficient catalyst for the selective oxidation of methane by oxygen

Dongli An, Qinghong Zhang, Ye Wang *

State Key Laboratory of Physical Chemistry of Solid Surfaces, National Engineering Laboratory for Green Chemical Productions of Alcohols, Ethers and Esters, College of Chemistry and Chemical Engineering, Xiamen University, Xiamen 361005, China

ARTICLE INFO

Article history:
Available online 20 February 2010

Keywords:
Methane
Selective oxidation
Oxygen
Formaldehyde
Copper catalyst
Grafting method

ABSTRACT

CuO_x/SBA-15 catalysts prepared by a grafting approach (denoted as CuO_x/SBA-15-*gra*) have been characterized and studied for the selective oxidation of methane to formaldehyde by oxygen. Our characterizations using XRD, H_2-TPR, UV–vis and ESR suggest that Cu^{2+} ions are almost isolated on the surface of SBA-15 at a Cu content $\leq$0.6 wt%. The increase in the Cu content to >0.6 wt% decreased the fraction of isolated Cu^{2+} ions and increased that of aggregated CuO_x clusters. On the other hand, the fraction of isolated Cu^{2+} ions was much smaller in the CuO_x/SBA-15 catalyst prepared by the impregnation method (denoted as CuO_x/SBA-15-*imp*) even with a lower Cu content (0.5 wt%). The CuO_x/SBA-15-*gra* provided significantly higher HCHO selectivity in the selective oxidation of CH_4 than the CuO_x/SBA-15-*imp*, and the CuO_x/SBA-15-*gra* catalyst with a Cu content of 0.6 wt% showed the best performance for HCHO formation. In situ FT-IR spectroscopy of adsorbed CO and XPS measurements suggest the generation of Cu^+ after the reaction, and the Cu^+ site is likely responsible for the activation of oxygen, forming an active oxygen species for the selective oxidation of CH_4 to HCHO.

1. Introduction

The selective oxidation of methane to useful oxygenates such as methanol and formaldehyde is one of the biggest challenges in catalysis. Two issues have made the selective oxidation of CH_4 quite challenging. First, because CH_4 is a very stable molecule, the activation of its C–H bond is not easy, and thus usually needs strict conditions. Second, and more importantly, the target products (CH_3OH and HCHO) are typically much more reactive than CH_4, and may easily undergo consecutive oxidations to carbon oxides (CO and CO_2). How to suppress the consecutive oxidation of more reactive products is also a critical challenge for many selective oxidation reactions.

Many heterogeneous catalysts have been reported for the selective oxidation of CH_4 to HCHO, and most of them are supported metal oxides (e.g., MoO_3/SiO_2 and V_2O_5/SiO_2) and composite metal oxides (e.g., $Fe_2(MoO_4)_3$ and $FePO_4$) [1–4]. However, these catalysts are still far from the commercial consideration because of the low productivity.

On the other hand, methane monooxygenases (MMOs) in methanotrophic bacteria can catalyze the selective oxidation of CH_4 to CH_3OH by O_2 under physiological temperature. Two types of MMO, i.e., soluble MMO (sMMO) and particulate MMO (pMMO) are known to exist, and the iron and copper centers dispersed in proteins are responsible for the selective oxidation of CH_4 in the sMMO and pMMO, respectively [5,6]. We believe that, the design of iron- or copper-containing heterogeneous catalysts with appropriate structure of active sites may be promising for the selective oxidation of CH_4. Several studies have contributed to the selective oxidation of CH_4 to HCHO with iron-based heterogeneous catalysts, and it is proposed that the high dispersion of Fe species is the key for obtaining high HCHO selectivity [4,7–14]. However, only very few reports have been contributed to the selective oxidation of CH_4 by O_2 over Cu-based heterogeneous catalysts. This is possibly because CuO is known to be an active catalyst for the complete oxidation of CH_4 to CO_2 [15], whereas in the pMMO, Cu sites are highly dispersed in the protein structure. Groothaert et al. [16,17] reported a stoichiometric reaction between the chemisorbed oxygen species on Cu-ZSM-5, possibly a bis(μ-oxo)dicopper species, $[Cu_2\text{-}(\mu\text{-}O)_2]^{2+}$, with CH_4 at $\geq$398 K, and they found the formation of CH_3OH. However, the reaction could not be operated in a catalytic manner.

Recently, we compared the catalytic performances of various transition metal ions or oxide clusters introduced into SBA-15, a typical mesoporous silica, with a low content (~0.01 wt%) by an impregnation method, and found that the supported CuO_x catalyst showed the best catalytic activity for HCHO formation [18]. This is a significant result because Cu sites are active centers in the

* Corresponding author. Fax: +86 592 2183047.
E-mail address: wangye@xmu.edu.cn (Y. Wang).

0920-5861/$ – see front matter © 2010 Elsevier B.V. All rights reserved.
doi:10.1016/j.cattod.2010.01.048

pMMO, whereas CuO is known to catalyze CH_4 combustion. We have examined the structure–performance correlation and clarified that the high dispersion of CuO_x species is a key point for HCHO formation [19]. However, by the impregnation method, CuO_x species began to aggregate to form oligomeric CuO_x clusters when the Cu content was larger than ~0.01 wt% over SBA-15 [19]. On the other hand, it was reported that isolated CuO_x moieties could be formed with a larger concentration by grafting organic copper precursors onto SBA-15 followed by calcination [20]. Recently, we have succeeded in preparing the CuO_x/SBA-15 catalysts with highly dispersed CuO_x species by a grafting method. The present paper reports the structural characteristics and the catalytic behaviors of the catalysts prepared by the grafting method.

2. Experimental

SBA-15 was synthesized in a hydrochloric acid medium using tetraethyl orthosilicate and a triblock copolymer ($EO_{20}PO_{70}EO_{20}$) as the silicon source and template, respectively [19]. After calcination to remove the organic template, SBA-15 with ordered hexagonal mesoporous channels was grafted with copper (II) acetylacetonate ($Cu(acac)_2$) using a method reported previously for the preparation of $Cu(acac)_2$-grafted activated carbon and HMS [21–23]. In brief, the mixture of pre-dried SBA-15 and γ-aminopropyl triethoxysilane was first refluxed in dry toluene under argon atmosphere to functionalize the surfaces of SBA-15 (Scheme 1). Then, $Cu(acac)_2$ was grafted onto the functionalized SBA-15 in dry toluene under reflux conditions under argon atmosphere for 24 h. Schiff condensation between the amine group attached on SBA-15 and the carbonyl group in the acetylacetonate ligand was proposed to occur [21–23]. The grafted material was recovered by filtration, followed by washing with toluene and drying at 323 K overnight. Finally, this material was calcined in air at 923 K for 6 h to remove the organic groups. Cu contents in all of the catalysts were analyzed by ICP method. For comparison, CuO_x/SBA-15 samples were also prepared by the conventional impregnation method (denoted as CuO_x/SBA-15-*imp*), and the detailed procedure was reported in our previous paper [19].

The catalysts were characterized by several spectroscopic techniques. XRD measurements were performed with a Panalytical X'pert Pro Super X-ray diffractometer with Cu K_α radiation (40 kV and 30 mA). Diffusion reflectance UV–vis spectra were recorded on a Varian-Cary 5000 spectrometer equipped with a diffuse reflectance accessory. The spectra were collected with $BaSO_4$ as a reference. H_2-TPR was performed using a Micromeritics AutoChem 2920 II instrument. Typically, a H_2–Ar gas mixture (5 vol% H_2) was introduced into the reactor, and the temperature was raised to 1073 K at a rate of 10 K min^{-1}. H_2 consumption was monitored by a thermal conductivity detector. EPR measurements were performed on a Bruker EMX EPR spectrometer at X-band frequency (9.46 GHz). Transmission FT-IR spectra of CO adsorption were recorded on a Nicolet FTIR 380 instrument equipped with an MCT detector with a resolution of 2 cm^{-1}. The sample was pressed into a self-supporting wafer and was placed in an in situ IR cell.

The catalytic reactions were performed on a fixed-bed quartz reactor operated at atmospheric pressure. The products were analyzed by on-line gas chromatography, and all the lines and values between the exit of the reactor and the gas chromatographs were heated to 393 K to prevent the condensation of products. The details of the procedures for reactions and product analyses were reported previously [13,19]. Unless otherwise stated, catalytic performances after 6 h of reactions (steady state) were described and discussed.

3. Results and discussion

3.1. Structure characteristics of the CuO_x/SBA-15 prepared by the grafting method

We have characterized the calcined CuO_x/SBA-15-*gra* samples with different Cu contents. Fig. 1 shows the XRD patterns at both low and high diffraction angles for these samples. Three diffraction peaks at 2θ degrees of ~1.0°, ~1.6° and ~1.9°, attributed to the (1 0 0), (1 1 0), and (2 0 0) reflections of hexagonal arrays of the mesoporous structure of SBA-15 [19], were observed for these CuO_x/SBA-15 samples (Fig. 1A), indicating that the ordered mesoporous structure were well sustained after the grafting of Cu species onto SBA-15. At high diffraction angles, no diffraction peaks except for that of amorphous silica framework (2θ = ~22°) were observed, suggesting that Cu^{2+} species may be well dispersed on the surfaces of SBA-15.

From the diffuse reflectance UV–vis results shown in Fig. 2, we observed one main absorption band at ~235 nm for the CuO_x/SBA-15 samples with Cu contents of 0.6–2.9 wt%. This band could be assigned to the charge transfer transition between the ligand O^{2-}

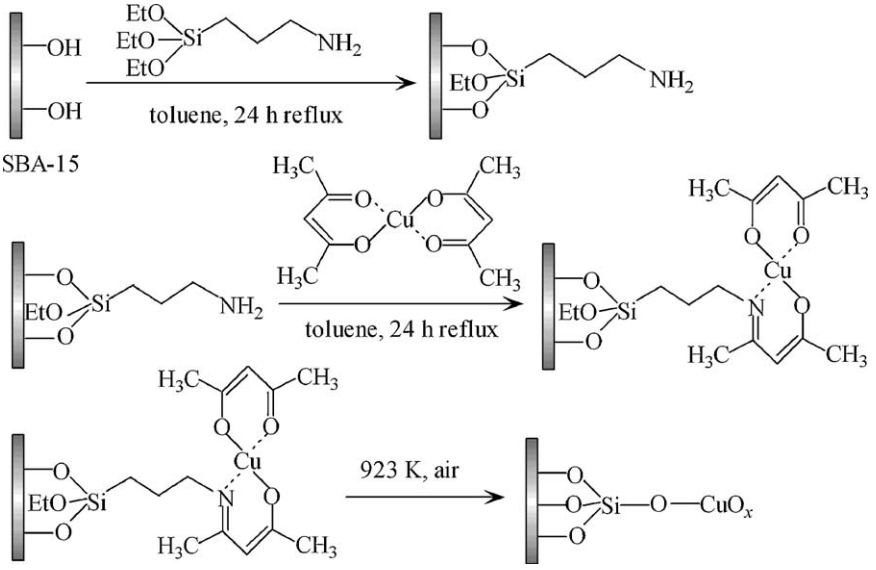

Scheme 1. Preparation of CuO_x/SBA-15 catalysts by the grafting method.

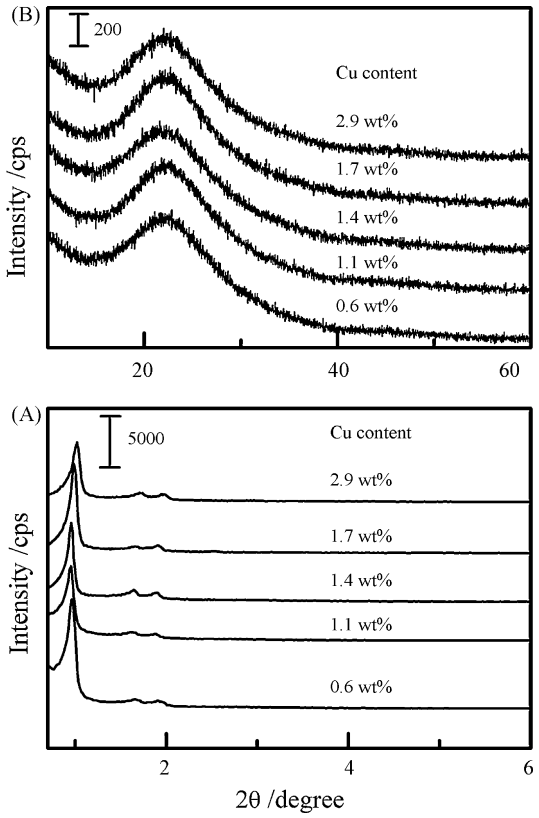

Fig. 1. XRD patterns of the CuO_x/SBA-15-*gra* catalysts with different Cu contents. (A) Low diffraction angles and (B) high diffraction angles.

and metal center Cu^{2+} in isolated state [24–26]. With increasing Cu content, a shoulder peak at about 290 nm was also observed, and this shoulder peak became distinct as the Cu content reached 2.9 wt%, indicating the presence of oligomeric CuO_x clusters in the samples with higher Cu contents [24–26]. These observations suggest that, after calcination, Cu^{2+} ions are highly dispersed on SBA-15 in the samples with lower Cu contents.

Fig. 3 shows the H_2-TPR profiles for the CuO_x/SBA-15 samples. It was reported that the isolated Cu^{2+} ions on SiO_2 prepared by an ion

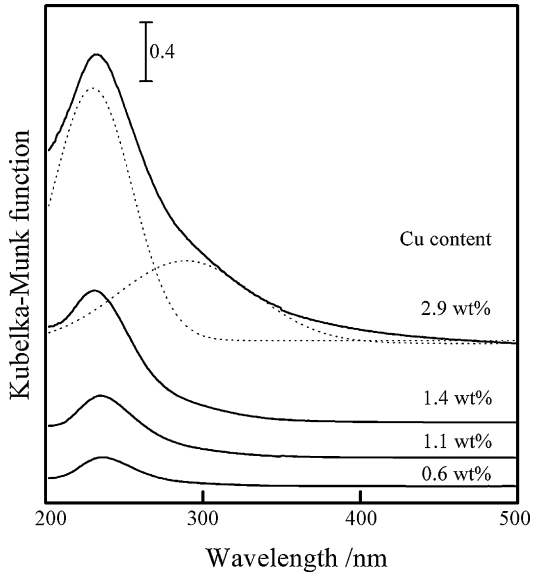

Fig. 2. Diffuse reflectance UV–vis spectra of the CuO_x/SBA-15-*gra* catalysts with different Cu contents.

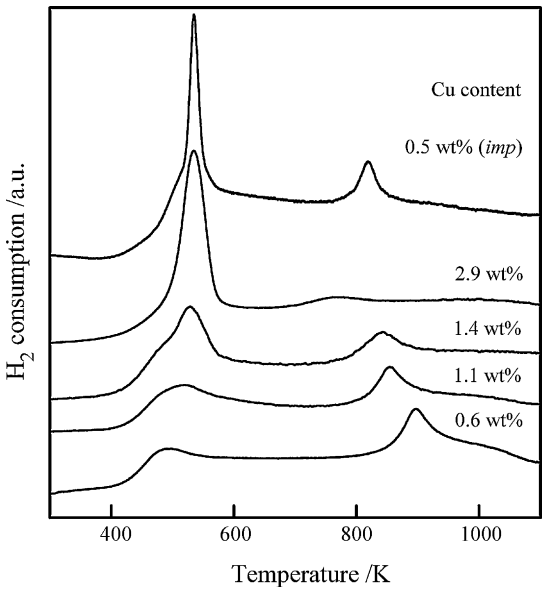

Fig. 3. H_2-TPR profiles of the CuO_x/SBA-15-*gra* catalysts with different Cu contents.

exchange method underwent a two-step reduction [27], i.e., the lower temperature peak was ascribed to Cu^{2+} to Cu^+, and the higher temperature peak to Cu^+ to Cu^0. Yamamoto et al. [28] also showed that the reduction of isolated Cu^+ species on Al_2O_3 occurred at significantly higher temperature than the reduction of Cu^{2+} or CuO. On the other hand, the aggregated CuO_x clusters typically show one reduction peak at the lower temperature region. Thus, it is reasonable to consider that the lower temperature peak in Fig. 3 corresponds to two contributions: (i) the one-step reduction of CuO_x clusters to Cu^0 and (ii) the partial reduction of isolated Cu^{2+} ions to Cu^+, while the higher temperature TPR peak corresponds to the second step reduction of Cu^+ to Cu^0 for the isolated copper species. From the relative intensity of the higher temperature peak, we have calculated the fraction of the isolated Cu^{2+} ions, and the results are shown in Table 1. It becomes clear that the sample with a Cu content of 0.6 wt% contains mainly isolated Cu^{2+} ions (96%), and the fraction of the isolated Cu^{2+} decreases with increasing the Cu content. We have carried out the same calculation for the 0.5 wt% CuO_x/SBA-15-*imp* prepared by the impregnation method. Although the Cu content was lower for this sample, the fraction of isolated Cu^{2+} was significantly lower (37%). This confirms that our present grafting method is effective for the preparation of highly dispersed copper species.

We have demonstrated that the EPR spectroscopy is a powerful tool for the characterization of Cu^{2+}-containing samples with low Cu contents [19]. From the EPR spectra for the present CuO_x/SBA-15-*gra* samples (Fig. 4), we obtained four splitting features ($m_I = -3/2, -1/2, +1/2, +3/2$) in the low-field region for the parallel component due to the hyperfine interaction between the unpaired electron and the nuclear spin of copper ($I = 3/2$), whereas the signal for the perpendicular component ($g_\perp = 2.08$) was nor

Table 1
Distribution of copper species in the CuO_x/SBA-15 catalysts.

Catalyst	Relative fraction of copper species[a] (%)	
	Isolated Cu^{2+} ions	Oligomeric CuO_x clusters
0.6 wt% CuO_x/SBA-15-*gra*	96	4
1.1 wt% CuO_x/SBA-15-*gra*	78	22
1.4 wt% CuO_x/SBA-15-*gra*	50	50
2.9 wt% CuO_x/SBA-15-*gra*	20	80
0.5 wt% CuO_x/SBA-15-*imp*	37	63

[a] Evaluated from H_2-TPR results.

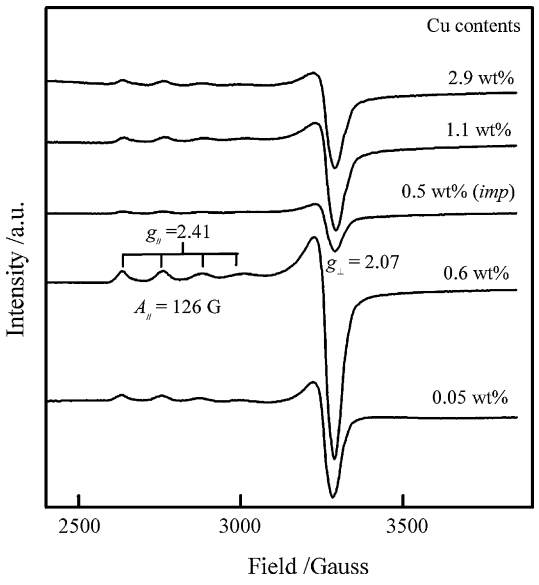

Fig. 4. EPR spectra of the CuO_x/SBA-15-*gra* catalysts with different Cu contents and the 0.5 wt% CuO_x/SBA-15-*imp*.

resolved. These characteristics are typical of isolated Cu^{2+} cations in axial symmetry [29]. The anisotropic parameters (g|| = 2.41, and A|| = 126 G) suggest that the Cu^{2+} cations are in octahedral coordination [30]. The intensity of EPR peaks increased significantly with increasing the Cu content from 0.05 to 0.6 wt%, but a further increase in Cu content to >0.6 wt% decreased the peak intensity. This decrease is probably due to the dipole–dipole interaction between neighboring Cu^{2+} species [31]. Thus, the decrease in EPR signal intensity suggests the aggregation of Cu^{2+} species to form oligomeric CuO_x clusters at Cu contents higher than 0.6 wt%. This is in agreement with the results obtained from H_2-TPR measurements (Table 1). The significant lower intensity of EPR signals for the 0.5 wt% CuO_x/SBA-15-*imp* sample further indicates that there is a smaller fraction of isolated Cu^{2+} in the sample prepared by the impregnation method.

3.2. Catalytic behaviors of the CuO_x/SBA-15 prepared by the grafting method

Catalytic performances changed with time on stream for our CuO_x/SBA-15-*gra* catalysts, and a steady state could be reached after 4–6 h for each catalyst. As an example, Fig. 5 shows the result

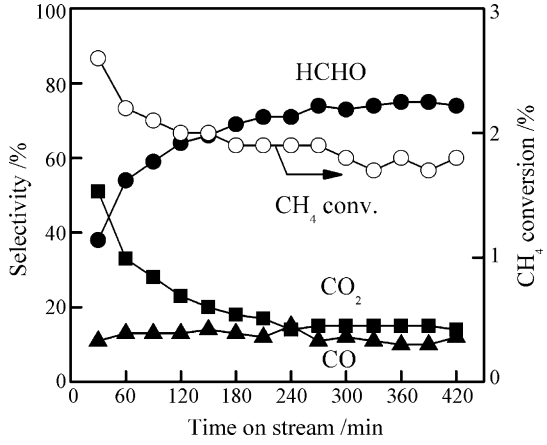

Fig. 5. Changes of catalytic performances with time on stream over the 0.6 wt% CuO_x/SBA-15-*gra* catalyst. Reaction conditions: W = 0.10 g, T = 898 K, $P(CH_4) = P(O_2)$ = 33.8 kPa, F(total) = 120 mL min^{-1}.

Table 2
Catalytic performances of CuO_x/SBA-15-*gra* catalysts with different Cu contents for the selective oxidation of CH_4 to HCHO[a].

Catalyst	CH_4 conv. (%)	Selectivity (%)			HCHO yield (%)
		HCHO	CO	CO_2	
SBA-15	0.30	96	0	4.0	0.29
0.05 wt% CuO_x/SBA-15	1.1	71	7.0	22	0.78
0.6 wt% CuO_x/SBA-15	1.8	71	11	18	1.3
1.1 wt% CuO_x/SBA-15	1.8	65	16	19	1.2
1.4 wt% CuO_x/SBA-15	2.2	50	20	30	1.1
1.7 wt% CuO_x/SBA-15	1.8	50	17	33	0.90
2.9 wt% CuO_x/SBA-15	2.4	36	13	51	0.86

[a] Reaction conditions: W = 0.10 g, T = 898 K, $P(CH_4) = P(O_2)$ = 33.8 kPa, F(total) = 120 mL min^{-1}.

for the 0.6 wt% CuO_x/SBA-15-*gra* catalyst. Thus, we use the data obtained after 6 h of reactions for discussion. Table 2 shows the catalytic performances of the CuO_x/SBA-15-*gra* catalysts with different Cu contents for the selective oxidation of CH_4 by O_2 at 898 K. Without loading copper, CH_4 conversion was low (0.3%) over SBA-15 alone. CH_4 conversion and HCHO yield increased significantly with increasing the Cu content, indicating that the copper species are responsible for the selective oxidation of CH_4 to HCHO by O_2. However, when the Cu content exceeded 0.6 wt%, the increase in CH_4 conversion became not significant. HCHO selectivity can keep at >70% at a Cu content ≤0.6 wt%. Further increases in the Cu content decreased the selectivity to HCHO, and increased that to CO_2 remarkably. The catalyst with a Cu content of 0.6 wt% afforded the highest HCHO yield (1.3%). The space time yield (STY) for HCHO formation can reach 28 mol kg_{cat}^{-1} h^{-1} over this catalyst at 898 K and a CH_4 partial pressure of 59 kPa, which is better than the best STY value for HCHO formation reported for the V_2O_5/SiO_2 catalyst [32]. Moreover, as compared to the Fe-doped SiO_2 catalysts [7–9], the present CuO_x/SBA-15-gra catalyst shows a significantly higher HCHO selectivity (>70%) at a reasonable CH_4 conversion (~2%).

To make a better comparison of catalytic performances among the CuO_x/SBA-15-*gra* catalysts with different Cu contents, we further carried out the reactions at different reaction temperatures. The results over the CuO_x/SBA-15-*gra* catalysts with different Cu contents were compared in the plot of HCHO selectivity versus CH_4

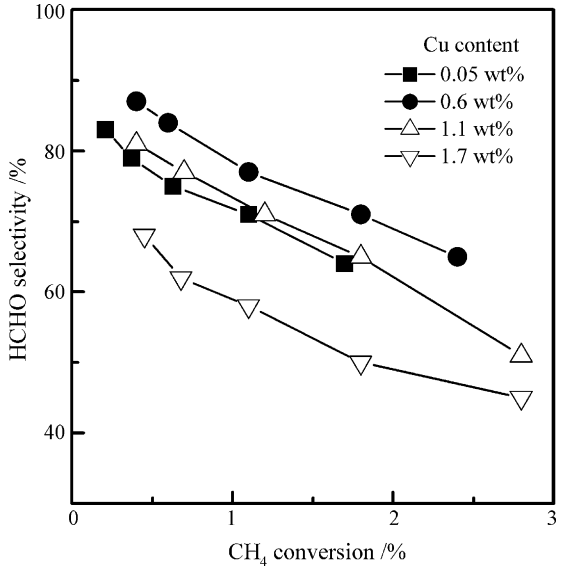

Fig. 6. HCHO selectivity as a function of CH_4 conversion for the CuO_x/SBA-15-*gra* catalysts with different Cu contents. Reaction conditions: W = 0.10 g, T = 823–898 K, $P(CH_4) = P(O_2)$ = 33.8 kPa, F(total) = 120 mL min^{-1}, time on stream = 10 h.

Table 3
Comparison of catalytic performances between CuO_x/SBA-15-*gra* and CuO_x/SBA-15-*imp* catalysts[a].

Catalyst	CH_4 conv. (%)	Selectivity (%)			HCHO yield (%)
		HCHO	CO	CO_2	
0.6 wt% CuO_x/SBA-15-*gra*	1.8	71	11	18	1.3
0.5 wt% CuO_x/SBA-15-*imp*	1.7	50	12	38	0.85
1.1 wt% CuO_x/SBA-15-*gra*	1.8	65	16	19	1.2
1.0 wt% CuO_x/SBA-15-*imp*	2.0	34	6	60	0.62

[a] Reaction conditions: $W = 0.10$ g, $T = 898$ K, $P(CH_4) = P(O_2) = 33.8$ kPa, $F(\text{total}) = 120$ mL min^{-1}.

conversion. As shown in Fig. 6, HCHO selectivity decreased with increasing CH_4 conversion by increasing the reaction temperature over each catalyst. HCHO selectivity over the 0.6 wt% CuO_x/SBA-15-*gra* catalyst was the highest if the comparison was made on the same CH_4 conversion level. This further demonstrates that the catalyst with a Cu content of 0.6 wt% provides the best performance for the selective oxidation of CH_4 to HCHO by O_2. From the dependence of CH_4 conversion rates on reaction temperature, we have calculated the activation energy for the CuO_x/SBA-15-*gra* catalysts with different Cu contents. The activation energies are 133, 118, 123, and 117 kJ mol^{-1} for the catalysts with Cu contents of 0.05, 0.6, 1.1, and 1.7 wt%, respectively.

We have compared the catalytic performances of the catalysts prepared by the grafting method with those by the impregnation method. Table 3 shows the results at 898 K over the two series of catalysts. As compared to the grafting catalysts with a similar Cu content, the impregnation catalyst exhibited significantly lower HCHO selectivity at a similar CH_4 conversion, whereas the selectivity to CO_2 was much higher.

3.3. Structure–performance correlation and possible reaction mechanism

As described above, we have clearly demonstrated that the CuO_x/SBA-15 catalysts prepared by the grafting method exhibit significantly higher selectivity than those prepared by the impregnation method. Moreover, the CuO_x/SBA-15-*gra* with a Cu content of 0.6 wt% affords the best catalytic performance for HCHO formation. Our characterizations using UV–vis, H_2-TPR and EPR suggest that the 0.6 wt% CuO_x/SBA-15-*gra* catalyst contains a very

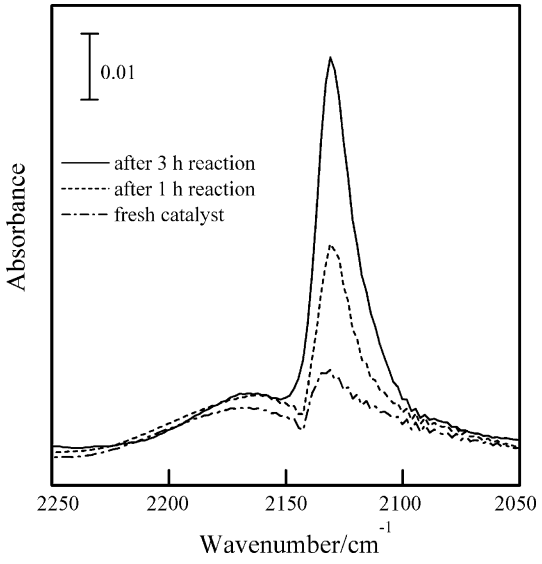

Fig. 7. In situ FT-IR spectra of adsorbed CO over the 0.6 wt% CuO_x/SBA-15-*gra* catalyst before and after reactions.

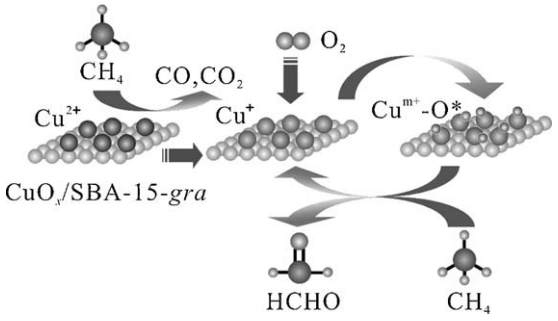

Scheme 2. Possible reaction mechanism for the selective oxidation of CH_4 to HCHO over the CuO_x/SBA-15-*gra* catalysts.

high fraction of isolated Cu^{2+} cations (96%). The fraction of isolated Cu^{2+} cations decreased and that of oligomeric CuO_x clusters increased with further increasing the Cu content. The CuO_x/SBA-15-*imp* catalyst contains a smaller fraction of isolated Cu^{2+} cations as compared to the CuO_x/SBA-15-*gra* catalyst with a similar Cu content. The correlation of the catalytic behaviors with the structure characteristics allows us to propose that the isolated Cu^{2+} cations account for the selective oxidation of CH_4 to HCHO by O_2, while the oligomeric CuO_x clusters are responsible for the oxidation of CH_4 to CO_2.

In our previous studies for the selective oxidation of CH_4 by O_2 over the CuO_x/SBA-15-*imp* catalysts with low Cu contents [19], we speculated that Cu^+ was generated from the isolated Cu^{2+} during the reaction, and was likely the active species for the selective oxidation of CH_4 to HCHO by O_2. However, we did not obtain direct evidence for Cu^+ because of the very low Cu content (0.008 wt%). Our present grafting catalysts possess higher Cu contents, and thus allow the characterization of the oxidation state of copper by several techniques. Fig. 7 shows the in situ FT-IR spectra of adsorbed CO over the 0.6 wt% CuO_x/SBA-15-*gra* before and after catalytic reactions under the conditions in Table 2. The adsorption of CO on the fresh catalyst only gave a very weak IR band, because Cu^{2+} sites did not adsorbed CO strongly [33]. After the reaction, the IR band at 2131 cm^{-1} was clearly observed and this band can be assigned to CO adsorbed on the Cu^+ sites. This band became stronger after a 3 h of reaction. These observations suggest that a part of Cu^{2+} cations has been reduced to Cu^+ during the reaction. XPS measurements for the 0.6 wt% CuO_x/SBA-15-*gra* catalyst before and after reactions showed that the binding energy of Cu $2p_{3/2}$ decreased from 933.3 to 932.5 eV, also indicating the partial reduction of Cu^{2+} to Cu^+ after the reaction. Therefore, we propose a reaction mechanism in Scheme 2 for the selective oxidation of CH_4 to HCHO over the CuO_x/SBA-15-*gra* catalysts. The isolated Cu^{2+} cations over our present catalysts are reduced into Cu^+ during the reaction, and the Cu^+ sites function for the activation of O_2 molecules, generating active oxygen species for the selective oxidation of CH_4 to HCHO. On the other hand, over the oligomeric CuO_x clusters, similar to the reaction over the supported CuO [15], the lattice oxygen may participate in the oxidation of CH_4, leading to complete oxidation to CO_2.

4. Conclusions

The grafting approach can provide CuO_x/SBA-15 catalyst with Cu^{2+} species highly dispersed on SBA-15. At Cu contents $\leq$0.6 wt%, the catalysts contain mainly isolated Cu^{2+} cations ($\geq$96%). The fraction of the isolated Cu^{2+} cations decreases and that of the oligomeric CuO_x clusters increases with increasing the Cu content to >0.6 wt%. The catalyst prepared by the grafting method possesses a significantly higher fraction of isolated Cu^{2+} cations than that prepared by the impregnation method. As compared to the catalyst prepared by the impregnation method, the CuO_x/SBA-

15-*gra* catalyst exhibits significantly higher HCHO selectivity on a similar CH_4 conversion level. The CuO_x/SBA-15-*gra* catalyst with a Cu content of 0.6 wt% demonstrates the best catalytic performance for HCHO formation. The isolated Cu^{2+} cations undergo partial reductions to Cu^+ sites during the reaction, and the Cu^+ sites are proposed for the activation of O_2, generating active oxygen species for the selective oxidation of CH_4.

Acknowledgements

This work was supported by the National Natural Science Foundation of China (Nos. 20625310, 20773099 and 20873110), the National Basic Program of China (2010CB732303 and 2005CB221408), and the Key Scientific Project of Fujian Province (2009HZ0002-1).

References

[1] J.H. Lunsford, Catal. Today 63 (2000) 165.
[2] K. Otsuka, Y. Wang, Appl. Catal. A: Gen. 222 (2001) 145.
[3] K. Tabata, Y. Teng, T. Takemoto, E. Suzuki, M.A. Bañares, M.A. Peña, J.L.G. Fierro, Catal. Rev.-Sci. Eng. 44 (2002) 1.
[4] A. Arena, A. Parmaliana, Acc. Chem. Res. 36 (2003) 867.
[5] M. Merkx, D.A. Kopp, M.H. Sazinsky, J.L. Blazyk, J. Müller, S.J. Lippard, Angew. Chem. Int. Ed. 40 (2001) 2782.
[6] S.I. Chan, K.H.-C. Chen, S.S.-F. Yu, C.-L. Chen, S.-J. Kou, Biochemistry 43 (2004) 4421.
[7] T. Kobayashi, K. Nakagawa, K. Tabata, M. Haruta, J. Chem. Soc. Chem. Commun. (1994) 1609.
[8] T. Kobayashi, N. Guihaume, J. Miki, N. Kitamura, M. Haruta, Catal. Today 32 (1996) 171.
[9] F. Arena, G. Gatti, G. Martra, S. Coluccia, L. Stievano, L. Spadaro, P. Famulari, A. Parmaliana, J. Catal. 231 (2005) 365.
[10] Q. Zhang, W. Yang, X. Wang, Y. Wang, T. Shishido, K. Takehira, Micropor. Mesopor. Mater. 77 (2005) 223.
[11] Y. Wang, W. Yang, L. Yang, X. Wang, Q. Zhang, Catal. Today 117 (2006) 156.
[12] Y. Wang, Res. Chem. Intermed. 32 (2006) 235.
[13] Q. Zhang, Y. Li, D. An, Y. Wang, Appl. Catal. A: Gen. 356 (2009) 103.
[14] J. He, Y. Li, D. An, Q. Zhang, Y. Wang, J. Nat. Gas Chem. 18 (2009) 288.
[15] P.W. Park, J.S. Ledford, Appl. Catal. B: Environ. 15 (1998) 221.
[16] M.H. Groothaert, P.J. Smeets, B.F. Sels, P.A. Jacobs, R.A. Schoonheydt, J. Am. Chem. Soc. 127 (2005) 1394.
[17] P.J. Smeets, M.H. Groothaert, R.A. Schoonheydt, Catal. Today 110 (2005) 303.
[18] Y. Li, S. Chen, Q. Zhang, Y. Wang, Chem. Lett. 35 (2006) 572.
[19] Y. Li, D. An, Q. Zhang, Y. Wang, J. Phys. Chem. C 112 (2008) 13700.
[20] I.J. Drake, K.L. Fujdala, A.T. Bell, T.D. Tilley, J. Catal. 230 (2005) 12.
[21] A.R. Silva, M. Martins, M. Madalena, A. Freitas, J.L. Figueiredo, C. Freire, B. de Castro, Eur. J. Inorg. Chem. (2004) 2027.
[22] A.R. Silva, J.L. Figueiredo, C. Freire, B. de Castro, Catal. Today 102–103 (2004) 154.
[23] A.R. Silva, K. Wilson, A.C. Wgitwood, J.H. Clark, C. Freire, Eur. J. Inorg. Chem. (2006) 1275.
[24] S. Velu, K. Suzuki, M. Okazaki, M.P. Kapoor, T. Osaki, F. Ohashi, J. Catal. 194 (2000) 373.
[25] L. Chmielarz, P. Kuśtrowski, R. Dziembaj, P. Cool, E.F. Vansant, Appl. Catal. B 62 (2006) 3369.
[26] Y. Wang, H. Chu, W. Zhu, Q. Zhang, Catal. Today 131 (2008) 496.
[27] E.D. Guerreiro, O.F. Gorriz, J.B. Rivarola, L.A. Arrúa, Appl. Catal. A: Gen. 165 (1997) 259.
[28] T. Yamamoto, T. Tanaka, R. Kuma, S. Suzuki, F. Amano, Y. Shimooka, Y. Kohno, T. Funabiki, S. Yoshida, Phys. Chem. Chem. Phys. 4 (2002) 2449.
[29] S.C. Larsen, A. Aylor, A.T. Bell, J.A. Reimer, J. Phys. Chem. 98 (1998) 11533.
[30] P. Decyk, Catal. Today 114 (2006) 142.
[31] F. Amano, T. Tanaka, T. Funabiki, J. Mol. Catal. A: Chem. 221 (2004) 89.
[32] A. Parmaliana, F. Frusteri, A. Mezzapica, M.S. Scurrel, N. Giordano, J. Chem. Soc. Chem. Commun. (1993) 751.
[33] K.I. Hadjiivanov, G.N. Vayssilov, Adv. Catal. 47 (2002) 307.